JNIRS

JOURNAL
OF
NEAR
INFRARED
SPECTROSCOPY

Special Issue: Near Infrared Spectroscopy of Soil

Visible and near infrared spectra of Ferralsols according to their structural features

José Francirlei de Oliveira,[a]* Michel Brossard,[b] Edemar Joaquim Corazza,[c] Robélio Leandro Marchão[d] and Maria de Fátima Guimarães[a]

[a]Universidade Estadual de Londrina (UEL), Centro de Ciências Agrárias (CCA), Departamento de Agronomia, Rodovia Celso Garcia Cid, PR 445, Km 380, CEP 86051-980, Londrina, PR, Brazil. E-mail: jfoliveira79@gmail.com

[b]IRD (Institut de recherche pour le développement), UMR 210 Eco&Sols, Campus SupAgro Bât. 12, Place Viala, 34060, Montpellier Cedex 2, France

[c]Embrapa Informação Tecnológica, CP-040315, CEP 70770-901, Brasília, DF, Brazil

[d]Embrapa Cerrados, CP-08223, CEP-73310-970, Planaltina, DF, Brazil

In soil science, structural features of soils are an important attribute; soils can be characterised by proportional size distribution of aggregates and the pore space between and within those aggregates. The objective of this study was to evaluate the relationship between the visible and near infrared (Vis-NIR) spectra and microaggregates from a collection of Ferralsols. Our dataset consists of 56 spectra from seven soil profiles of kaolinitic and oxidic–gibbsitic Ferralsols. Soils were characterised according to their morphological features: those with a typical porous massive structure and those with a cohesive massive structure. Size distribution of five classes of microaggregate was determined (1000–2000 µm, 500–1000 µm, 250–500 µm, 105–250 µm and <105 µm). From the soil spectra, we determined the CIE (Commission Internationale de l'Eclairage) red index (RI_{CIE}) and the absorption intensities of kaolinite (I_{Ka}) and gibbsite (I_{Gb}). The predominant fraction of microaggregates exhibited sizes between 250 and 1000 µm ($\Phi_{250-1000}$). The proportional increase of this microaggregate class in the soils increased the scattering and variability of reflected light, particularly when soil samples showed more than 0.50 g g^{-1} of $\Phi_{250-1000}$. The microaggregate size explained over 55% of reflectance intensity variability of wavelengths in the Vis-NIR regions, principally on reflectance intensity and concavity of the spectra at 436 nm, 546 nm and 2236 nm, which decreases with increased proportion of $\Phi_{250-1000}$. Thus, different structural features of Ferralsols can be directly evaluated through Vis-NIR spectroscopy, even in samples sieved through 2.00 mm. These results highlight the potential use of Vis-NIR spectroscopy in studies of soil classification, soil physical behaviour and soil physical fertility and environmental studies, principally by a new method of analysing bulk density and structure of soil directly from the soil spectra, without the need for predictive models. As well as spectra, RI_{CIE}, I_{Ka} and I_{Gb} can be used to characterise the various structural features of Ferralsols.

Keywords: diffuse reflectance spectroscopy, Latosol, soil structure, microped, soil mineral

Introduction

Diffuse reflectance spectroscopy in the visible and near infrared (Vis-NIR) has been widely used in soil science, particularly during the last two decades.[1–3] In the first Vis-NIR studies, several pre-treatments were applied to obtain representative spectra of soils, including the sieving of samples to reduce the particle size effect. Thus, the collection of spectra

in the Vis-NIR region was performed using samples with sizes of less than 2 μm, with diameters smaller than the wavelength involved in the analysis.[1] However, due to the evolution of computers and spectrometers and to the important contribution of Norris and Hart[4] and Ben-Gera and Norris,[5] the collection of soil spectra is able to be performed on samples sieved at 2000 μm, without any other pre-treatment.

Soil contains solid particles that differ in size; soil science classifies three principal classes of particles: sand (0.05–2 mm), silt (0.002–0.05 mm) and clay (<0.002 mm). These particles are usually bound together as structural units called microaggregates, aggregates or peds according to their size. Among soils that present a microaggregated structure, there are Ferralsols,[6] Latosols of the Brazilian soil classification.[7] They typically have a strong microstructure.[8,9] Microaggregates are near spherical, usually ranging from 80 μm to 1000 μm in size. They correspond to the "pseudosand", "micropeds" and "granules" previously described by Kubiena,[10] Brewer[11] and Trapnell and Webster,[12] respectively. The size, development and arrangement of these aggregates and the distribution of pore space between and within the aggregates characterise soil structure. As far as soil structural differentiation is concerned, Ferralsols show a B horizon characterised by a moderate to weak macrostructure and a strongly developed granular fine to very fine microstructure.[13] The organisation and stability of Ferralsol microaggregates are dependent on the concentration of resistant minerals (e.g. quartz), along with principally iron and aluminium oxides and kaolinite.[6] This mineralogy explains the shape, features and stable microstructure. Soil colour is defined by the proportion of iron oxides, yellowish with goethite or reddish with hematite, according to the organic matter content. The oxidic Ferralsols are organised into microaggregates of less than 1 mm in size, with *in situ* porous massive macromorphological characteristics, and kaolinitic Ferralsols are organised into nodules surrounded by a dense and continuous plasma with cohesive massive macromorphological characteristics.[14] Volland-Tuduri[15] noted that Ferralsols might exhibit up to four types of microaggregate, with diameters that vary from 50 μm to 500 μm, promoting significant variations in inter- and intra-aggregate porosity according to their proportions, as also observed by Balbino et al.[16]

Reflectance obtained by satellite images or by laboratory equipment is inversely proportional to the particle diameter and microroughness of a sample.[1,17–19] Reflectance values depend on soil aggregates and how they are organised to form the structure, which is characterised by its millimetric roughness, directly influencing the scattering of light in the spectrometer.[3,8–10] Additionally, Chang et al.[20] observed an accuracy of Vis-NIR spectra in samples with similar particle sizes. Using samples of four soil types, including a red Ferralsol, Wu et al.[18] observed that sample size and roughness changed the region of spectral peaks, particularly those near the 2350 nm region. Chamizo et al.[21] observed that diffuse reflectance spectroscopy discriminated soil biological

aggregates and Croft et al.[22] reported that it was possible to characterise the roughness of different soil samples with spectra from the 400–2500 nm region. In the NIR region it was possible to distinguish aggregates according to their origin, soil, eroded material and biological aggregates.[23] In this way, different Ferralsols may promote a specific light variability for each soil macromorphology. This is because the shapes and features of microaggregates associated with organic matter and iron and aluminium oxy-hydroxides significantly affect wavelengths in the visible region, especially at 700 nm, 546 nm and 436 nm that represent the balance between red, green and blue colours (spectral bands known as red index of soil, RI_{CIE}), and 2200 nm and 2300 nm which are strongly linked to the absorption intensity of kaolinite and gibbsite, respectively. These facts explain why the relations between soil colour and spectra have been studied in the last fifty years.[24–26]

Macromorphological soil features are important for soil classification, soil physical behaviour, soil physical fertility and environmental studies. We consider that different macromorphological features may promote diverse spectra according to the shapes and features of the aggregates. This effect has not been investigated in natural microaggregates and the link between the spectra and existing microaggregates in soil samples sieved at 2000 μm is not clear. Therefore, the objective of this study was to evaluate the Vis-NIR spectra of soil in relation to microaggregates from a collection of Ferralsols with various mineralogy.

Materials and methods
Sample collection and soil characterisation

Seven Ferralsol profiles developed on meta-sedimentary rock composed of mudstones were collected from the central plateau, Brazil (Goiás state, 15°22′S and 47°27′W) and used in the present study. The soils were classified according to the Brazilian soil classification system[7] as Acric Red–Yellow Latosol, Dystrophic Red Latosol, Alic Red–Yellow Latosol and Dystrophic Red–Yellow Latosol (Table 1). Soils were described according to the field manual of Santos et al.[27] and the colour of the dry soil was determined using the Munsell chart[28] as reported previously.[29]

All samples were collected in triplicate from soil profiles at the following depths: 0.00–0.05 m, 0.05–0.10 m, 0.125–0.175 m, 0.225–0.275 m, 0.325–0.375 m, 0.725–0.775 m, 0.875–0.925 m and 1.075–1.125 m. The disturbed samples were air-dried and sieved at 2 mm. All samples exhibited 100% fine earth.

The physical and chemical analyses of samples were performed according to Donagema et al.[30] In brief, soil bulk density was determined by the cylinder method (94.16 cm^3); clay fraction was determined by the pipette method using 1 N NaOH as a chemical dispersant; organic matter content was determined by the Walkley–Black method; silica (SiO_2), iron (Fe_2O_3), aluminium (Al_2O_3) and titanium (TiO_2) were extracted by the sulphuric acid digestion method after dissolution in 1:1

Table 1. Main attributes of top (0.05–0.10 m) and lower (0.875–0.925 m) soil profile layer samples.

Soil profile	Soil classification[a]	Horizons	Colour	Compound structure[b]	D_b (g cm^{-3})	Particle size distribution [g kg^{-1}]			Organic matter (g kg^{-1})	SiO$_2$ (g kg^{-1})	Al$_2$O$_3$ (g kg^{-1})	Fe$_2$O$_3$ (g kg^{-1})	TiO$_2$ (g kg^{-1})	K_i	K_r
						<2 µm	2–50 µm	50–2000 µm							
L1	RYL Acric	Ap	5 YR 4/6	3fSBK and 3vfSBK and 3vfGR	0.91	842	99	58	34.15	185	240	101	26	1.31	1.03
		Bw1	5 YR 4/6	3vfGR and 1fSBK	0.88	802	149	47	8.58	226	260	110	36	1.48	1.16
L4	RL Dystrophic	Ap	5 YR 3/4	3mSBK and 3fSBK	0.88	794	98	108	26.11	125	285	96	41	0.75	0.61
		Bw	2.5 YR 4/8	3vfGR	0.87	878	32	90	7.52	196	275	95	38	1.21	0.99
L5	RYL Alic	Ap	7.5 YR 3/4	Massive and 1mSBK and 1fSBK	1.24	263	129	604	22.34	86	130	44	11	1.12	0.93
		Bw2	5 YR 3/4	Massive and 1mSBK	1.13	295	139	560	3.39	87	140	42	11	1.06	0.89
L7	RYL Alic	Ap	5 YR 3/2	Massive and 1mSBK and 2fSBK	1.06	351	196	449	23.58	111	151	40	11	1.25	1.07
		Bw1	5 YR 4/3	Massive	0.95	397	172	428	6.47	128	178	40	13	1.22	1.07
L8	RYL Alic	Ap	5 YR 3/3	2fSBK and 2vfSBK and Massive	1.04	344	168	484	24.84	85	172	55	12	0.84	0.70
		Bw1	2.5 YR 3/6	Massive	1.05	407	118	469	6.47	72	210	62	18	0.58	0.49
L9	RYL Dystrophic	Ap	7.5 YR 4/8	3fSBK and 1vfSBK	1.14	556	190	250	19.90	135	225	90	22	1.02	0.81
		Bw1	5 YR 4/6	Massive and 1fSBK and 1vfSBK	1.03	604	286	109	5.43	88	210	98	19	0.71	0.55
L11	RYL Alic	Ap	10 YR 4/3	3fSBK and 3mL and 3fL	1.24	462	289	249	15.21	165	197	41	19	1.42	1.26
		Bw2	7.5 YR 4/4	Massive	1.07	516	293	191	5.43	176	206	40	24	1.45	1.29

[a] According to Chang *et al.*,[20] RYL, red yellow latosol; RL, red latosol.

[b] Structure description (grade – size – type). Grade: 1 = weak; 2 = moderate; 3 = strong. Size of granular structure: vf = very fine (<1 mm); f = fine (1–2 mm); m = medium (2–5 mm); c = coarse (5–10 mm); vc = very coarse (>10 mm). Size of subangular blocky: vf = very fine (<5 mm); f = fine (5–10 mm); m = medium (10–20 mm); c = coarse (20–50 mm); vc = very coarse (>50 mm). Type: GR = granular; SBK = subangular blocky.

H_2SO_4; and silica, iron, aluminium and titanium contents were determined by inductively coupled plasma spectrometry. Silica and aluminium contents were used to calculate kaolinite and gibbsite contents, assuming that no isomorphic substitution occurs in these minerals.[31] To calculate the goethite and hematite contents, 33% and 16% aluminium substitutions were assumed, respectively.[32]

The SiO_2, Fe_2O_3 and Al_2O_3 contents, which were determined after extraction with sulphuric acid, were used to calculate the K_i and K_r ratios as follows:[33]

$$K_i = \frac{(SiO_2)/60}{(Al_2O_3)/102} = 1.7 \times \frac{SiO_2}{Al_2O_3}$$

$$K_r = \frac{(SiO_2)/60}{[(Al_2O_3)/102]+[(Fe_2O_3)/160]} = 1.7 \times \frac{SiO_2}{(Al_2O_3)+0.6375(Fe_2O_3)}$$

Fractionation of microaggregates in air-dried soil samples

Particle-size fractionation of microaggregates of <2000 μm was carried out using samples from the 0.875–0.925 m layer of seven profiles: L1, L4, L5, L7, L8, L9 and L11[29] (Table 1).

After reproducibility tests, air-dried soil samples (30 g; <2000 μm) were sieved through 2.00, 1.00, 0.50, 0.25 and 0.105 mm sieves for 30 s with mechanical agitation in a horizontal position, according to Volland-Tuduri.[15] After correcting for water contents (105 °C), the 1000–2000 μm, 500–1000 μm, 250–500 μm, 105–250 μm and <105 μm particle-size classes were determined. A linear equation based on the relation between Φ, greater proportion of microaggregates, and the inverse bulk density was generated, taking into account the relationship between macro- and microaggregates proposed by Volland-Tuduri et al.[34] (Figure 1).

This equation ($\Phi_{250-1000} = 0.608(1/D_b) - 0.113$) was used to determine parameter Φ for the other seven soil depths:
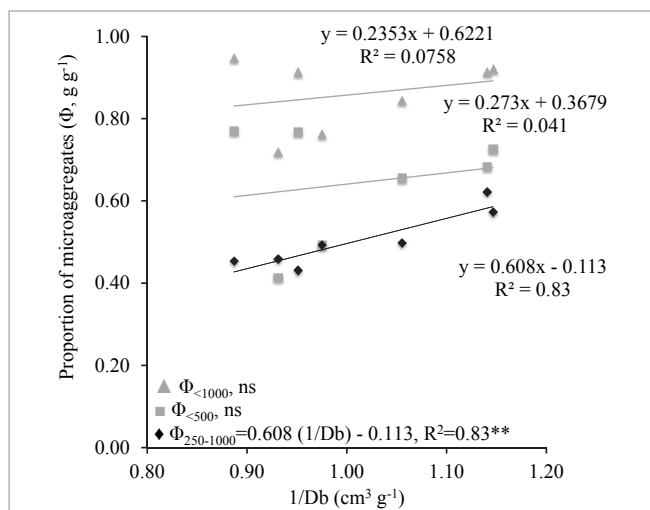
Figure 1. Correlation between the reciprocal of soil bulk density and the mass proportion of microaggregates with size <1000 μm ($\Phi_{<1000}$), <500 μm ($\Phi_{<500}$) and 250–1000 μm ($\Phi_{250-1000}$, n = 7) fraction. ns, non-significant correlation ($p < 0.05$).

0.00–0.05 m, 0.05–0.10 m, 0.125–0.175 m, 0.225–0.275 m, 0.325–0.375 m, 0.725–0.775 m and 1.075–1.125 m (n = 56).

Vis-NIR analyses
Sample preparation and spectra collection
Spectra were collected from 5 g of each soil sample (<2000 μm samples from the eight layers of soil profiles) packed into a cup with a 0.05 m diameter quartz lens; the samples were previously dried at 40 °C for 24 h and maintained in desiccators until the time of collection of the spectra to standardise their water content. Reflectance was determined at 2 nm intervals in the Vis-NIR region between 400 nm and 2500 nm using a FOSS XDS near infrared rapid content analyser (www.foss.dk), resulting in 1050 points for spectra.

The spectral variability was evaluated by repeating measurements 30 times on one soil sample, which was randomly selected. To perform each new scan, the ring cup was removed from the equipment and a new sample was prepared for the next replicate. The reflectance amplitudes of these readings ranged from 0.008 nm to 0.01 nm (95% probability). Therefore, variations larger than 0.01 nm between the spectra of different soil profiles were considered to be due to the sample, and no residual effect due to the equipment was observed. Each spectrum sample represented an average of 32 readings. The average spectrum from three repetitions for each layer of the soil profiles was obtained using WinISI II v1.50 software (Foss NIRSystems/Tecator Infrasoft International LLC, Silver Spring, MD, USA).

Spectral attributes
According to the CIE (Commission Internationale de l'Eclairage) the red index (RI_{CIE}) considers the wavelengths 700 nm for red (R), 546 nm for green (G) and 436 nm for blue (B) to represent the visible spectrum region. This colorimetric parameter, which is derived from the diffuse reflectance, is related to the hematite content and to the hematite/goethite ratio in the soil.[24,25] RI_{CIE} was calculated according to the following equation:

$$RI_{CIE} = \frac{(x-0.32)^2 \times 10,000}{(y-0.32) \times Y^2}$$

where x and y correspond to the chromaticity coordinates of the Munsell colour chart[28] and Y to the light intensity based on the standard observer determined by the CIE in 1931, using standard D65 lighting. Chromaticity coordinates were derived from the trichromatic components (X, Y and Z) and calculated according to Madeira Netto.[35]

Absorption intensities of kaolinite and gibbsite were used to analyse the effects of microaggregate grain size classes on the spectra because Madeira Netto et al.[36] observed that absorption intensities of kaolinite and gibbsite had a better correlation with the spectra than did the contents of these minerals.

The point of maximum reflectance between wavelengths 2200 nm and 2300 nm was chosen to calculate the absorption

intensities of kaolinite (I_{Ka}) and gibbsite (I_{Gb})[36] using the following equations:

$$I_{Ka} = R_{max} - R_{2205}$$

$$I_{Gb} = R_{max} - R_{2265}$$

where R_{max} is the maximum reflectance between 2205 nm and 2265 nm, and R_{2205} and R_{2265} are the reflectances at 2205 nm and 2265 nm, respectively. The ratio between the absorption intensities of these minerals was calculated using the equation $I_{Ka}/(I_{Ka} - I_{Gb})$.

Statistical analyses

The effect of the microaggregates on the spectra was assessed using linear regression analyses and the Pearson correlation ($p < 0.01$). To better represent the correlations with the components of the soil, the reflectance R in the correlation matrix was transformed into an absorbance value using the equation $A = \log_{10}(1/R)$. The 401 nm, 436 nm, 440 nm, 530 nm, 546 nm, 550 nm, 650 nm, 700 nm, 845 nm, 850 nm, 870 nm, 901 nm, 931 nm, 951 nm, 1051 nm, 1302 nm, 1401 nm, 1903 nm, 2201 nm, 2236 nm, 2263 nm, 2300 nm, 2352 nm and 2430 nm wavelengths were used in the correlation matrix to confirm the effects of microaggregates on the spectra; significant coefficients greater than 0.5 ($p < 0.05$) were considered. These wavelengths were selected because of their interactions with phyllosilicates (1:1), iron and aluminium oxy-hydroxides and organic matter[25,26,36,37] and allowed the discrimination of different soils according to their spectra.[38]

Following their field description, the superficial (0.05–0.10 m) and subsurface (0.875–0.925 m) layers of the soils were grouped according to their macromorphological descriptions for a comparison of variables related to the proportion of microaggregates characterised by factor $\Phi_{250-1000}$ and to the spectra (RI_{CIE}, I_{Ka} and I_{Gb}). The data were subjected to the Kruskal–Wallis test[39] at 5% probability.

Results
Soils studied

In terms of soil morphology, a subangular block structure on the surface and a strong granular and very thin structure in the layers below 0.72 m were observed, with *in situ* porous massive macromorphological characteristics in L1 and L4 profiles and with cohesive massive macromorphological characteristics in L5, L7, L8, L9 and L11 profiles (Table 1).

For the seven soil profiles, the clay content ranged from 263 g kg^{-1} to 878 g kg^{-1}, the iron oxide content ranged from 40 g kg^{-1} to 110 g kg^{-1} and the hue ranged from 2.5 YR to 10 YR. The K_i and K_r values of the surface layer were greater than 0.75 for L1, L4, L5, L7 and L11 soils and less than 0.75 for L8 and L9 soils (Table 1).
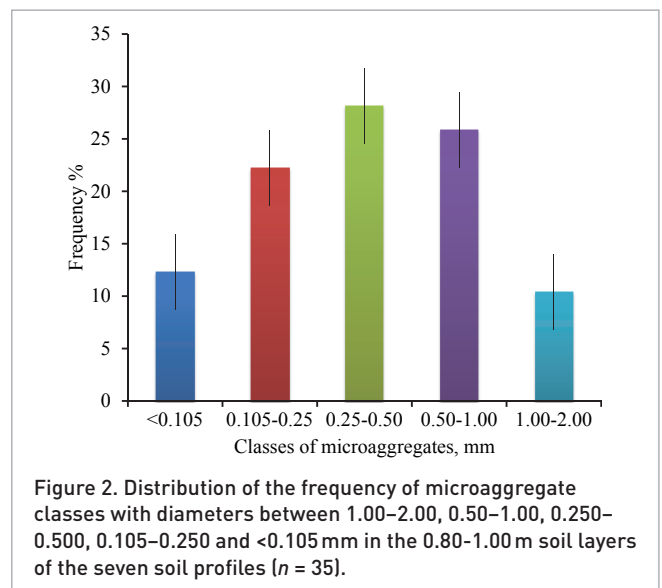
Figure 2. Distribution of the frequency of microaggregate classes with diameters between 1.00–2.00, 0.50–1.00, 0.250–0.500, 0.105–0.250 and <0.105 mm in the 0.80-1.00 m soil layers of the seven soil profiles ($n = 35$).

Particle size distribution of microaggregates (Φ)

The Φ of the greatest proportion was from the 250–1000 µm class ($\Phi_{250-1000}$) that varied from 0.38 g g^{-1} to 0.58 g g^{-1} of soil (Figure 2).

L1 and L4 soils, with porous massive structures, exhibited 29% higher $\Phi_{250-1000}$ on average compared with L5, L7, L8, L9 and L11 soils, which had cohesive massive structures. This difference was significant (Table 2) and confirmed previous macromorphological soil descriptions.

Soil spectra

The mean spectra of the surface and subsurface layers of the seven soil profiles were described in Oliveira *et al.*[29]J.F. We observed five bands of reflectance at 400–550 nm, 700–850 nm, 1350–1450 nm, 1850–2000 nm and 2200–2300 nm [Figure 3(a)].

We observed that bands of cohesive massive structure profiles (L5, L7, L8, L9 and, especially, L11) from the 0.80–1.00 m layer of the seven soils presented a narrow spectral band with greater reflectance intensity than soils L1 and L4 with porous massive structure [Figure 3(b)]. The concavity of the spectral band and the reflectance intensity at wavelengths of 436 nm, 546 nm and 700 nm were related to the proportion of microaggregates. The increase in proportion of $\Phi_{250-1000}$ was associated with a decrease in the reflectance intensity and an increased concavity of the spectra [Figure 3(b)].

Likewise, it was observed that reflectance intensity between 2200 nm and 2300 nm was related to $\Phi_{250-1000}$, given that soils with cohesive massive structure (L5, L7, L8, L9 and, particularly, L11) presented greater reflectance intensity at 2265 nm than L1 and L4 soils with porous massive structure [Figure 3(c)].

Relationship between wavelengths and soil morphology

Soil macromorphology, represented by proportion of $\Phi_{250-1000}$, was correlated with wavelengths between 400 nm and

Table 2. Microstructural and spectral characteristics of soil layer surface (0.05–0.10 m) and subsurface (0.875–0.925 m), based on morphological structures.

Soil profile	Horizons	$\Phi_{250\text{-}1000}$ (g g^{-1})	RI_{CIE}	I_{Ka}	I_{Gb}
Porous massive structure					
L1	Ap	0.56	0.77	0.14	0.1
	Bw1	0.58	1.05	0.07	0.02
L4	Ap	0.58	1.03	0.17	0.12
	Bw	0.58	1.44	0.12	0.05
Mean		0.58	1.07	0.13	0.07
CV%		1.74	25.75	33.63	63.08
Cohesive massive structure					
L5	Ap	0.38	0.24	0.33	0.33
	Bw2	0.43	0.31	0.34	0.34
L7	Ap	0.46	0.52	0.31	0.32
	Bw1	0.53	0.62	0.31	0.32
L8	Ap	0.47	0.48	0.28	0.28
	Bw1	0.47	0.58	0.29	0.29
L9	Ap	0.42	0.19	0.23	0.21
	Bw1	0.48	0.21	0.27	0.24
L11	Ap	0.38	0.2	0.32	0.35
	Bw2	0.45	0.18	0.33	0.38
Mean		0.45	0.35	0.30	0.31
CV%		10.34	50.13	11.23	16.89
H		8.10	8.00	8.03	8.01
p-value		<0.01	<0.01	<0.01	<0.01

2430 nm (Table 3), except for the 650 nm and 700 nm wavelengths. The predominant proportion of microaggregates in these Ferralsols accounted for over 55% of reflectance variability at wavelengths between 436 nm and 546 nm and over 65% for wavelength of 2236 nm. Reflectance intensity at these wavelengths decreased with an increase in proportion of $\Phi_{250\text{-}1000}$ [Figure 3(d)]–(f)].

Microaggregates were related to RI_{CIE} and to the absorption intensity of kaolinite and gibbsite (Table 3). L1 and L4 soils, with higher proportions of $\Phi_{250\text{-}1000}$, exhibited higher RI_{CIE} values and lower I_{Ka} and I_{Gb} values than the cohesive massive structure profiles. These differences were significant (Table 2). In the region of 400 nm to 730 nm, the increase in proportion of $\Phi_{250\text{-}1000}$ intensified the RI_{CIE} absorption [Figure 4(a)]. Furthermore, in the NIR region in soils with cohesive massive structures, the increase in $\Phi_{250\text{-}1000}$ did not result in increased variability of the ratio $I_{Ka}/(I_{Ka} + I_{Gb})$, in contrast to the porous massive structure soils whose variability was more obvious [Figure 4(b)]. Thus, the variability between I_{Ka} and I_{Gb} ratio, at wavelengths between 2200 nm and 2300 nm, increased when $\Phi_{250\text{-}1000}$ was greater than 0.50 g g^{-1} of soil.

RI_{CIE} was negatively related to total iron oxides ($R^2 = -0.55$; $p < 0.01$), in particular with goethite contents ($R^2 = -0.53$; $p < 0.01$), and this relationship occurred throughout the 401–1051 nm wavelength range (R^2 between 0.48 and 0.69; $p < 0.01$). I_{Ka} exhibited a negative correlation with the kaolinite content of the soil ($R^2 = -0.65$; $p < 0.01$), despite the positive correlation for wavelengths between 2200nm and 2300 nm with the contents of this mineral (R^2 between 0.58 and 0.66; $p < 0.01$). I_{Gb} exhibited a stronger negative correlation with goethite content ($R^2 = -0.84$; $p < 0.01$) than with gibbsite content ($R^2 = -0.04$; not significant).

We observed that the effect of microaggregates on wavelengths between 401 nm and 2430 nm hindered but did not prevent the observation of the link between attributes of the spectra and soil. However, on the other hand, the link between microaggregates and spectra showed the potential of Vis-NIR spectra for discriminating soils according to their morphology.

Discussion
Spectra related to soil structure

Morphological characteristics of Ferralsol microaggregates examined in this study were not altered after the manual breakdown of the clumps and subsequent sieving through 2 mm mesh (as verified with a magnifying glass), which allows the effect of these microaggregates on the scattering of light and noise from the Vis-NIR spectra to be discussed.
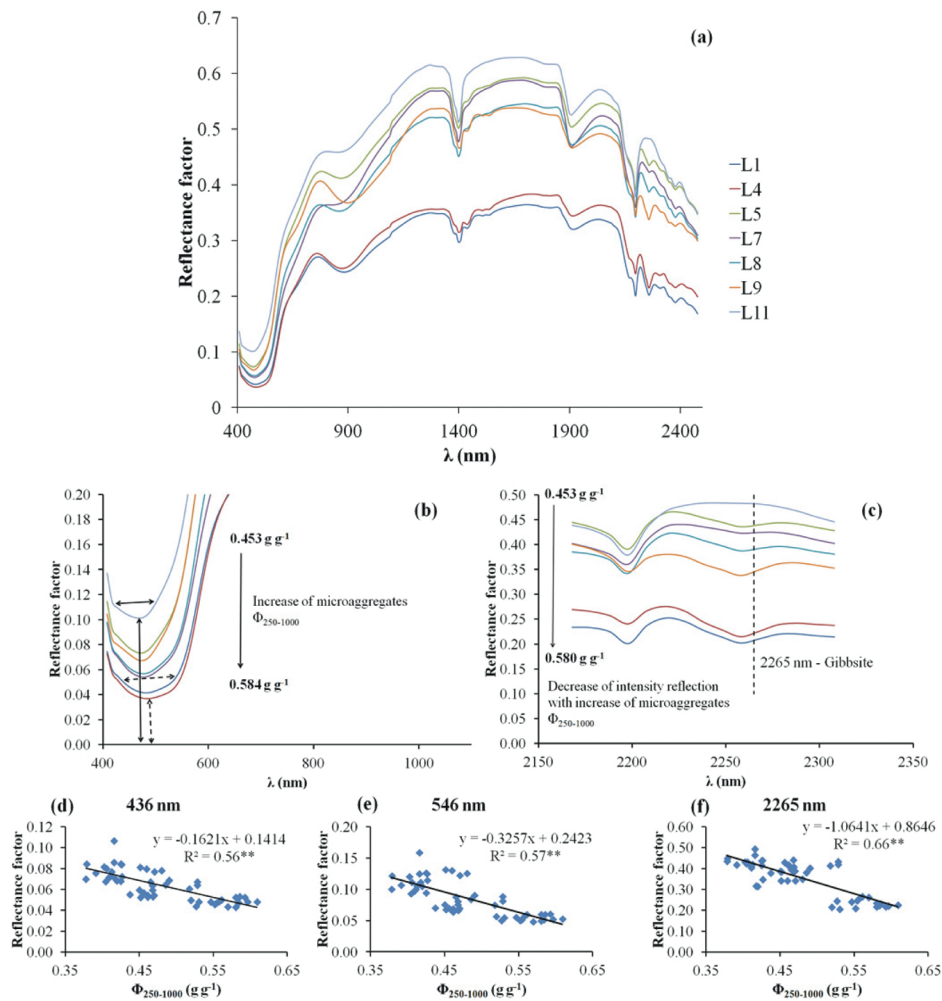
Figure 3. (a) Soil sample spectral mean reflectance from 400 nm to 2500 nm (0.875–0.925 m layer); (b) spectrum expansion at wavelengths between 400 nm and 770 nm, indicating reflectance intensity and concavity according to microaggregates; (c) spectrum expansion at wavelengths between 2200 nm and 2300 nm, indicating the reflectance intensity according to microaggregates. Linear regression between microaggregate size range 250–1000 µm ($\Phi_{250-1000}$) and wavelengths (d) 436 nm, (e) 546 nm and (f) 2265 nm. In (b) the dashed line indicates wide spectral band with lower intensity of reflectance and the solid line indicates narrow spectral band with greater intensity of reflectance.

All wavelengths analysed were correlated with microaggregates of size in the range 250–1000 µm, except 650 and 700 nm (Table 3). The increased proportion of $\Phi_{250-1000}$ of these Ferralsols explained over 55% of the reflectance intensity variability of wavelengths 436 nm, 546 nm and 2236 nm and the reflectance intensity. The concavity of the spectra at these wavelengths decreased with an increased proportion of these microaggregates [Figure 3(d)–(f)].

These results can be explained by two effects of microaggregates on light reflection. The first effect is that the proportional mass increase of $\Phi_{250-1000}$ intensifies the scattering process of light, particularly at 436 nm and 546 nm in the visible region and at 2236 nm in the NIR [Figure 3(b), (d) and (e)]. In the NIR region, at 2200–2300 nm, the scattering process caused by microaggregates is more pronounced in soils with porous massive structure (L1 and L4), with $\Phi_{250-1000}$ of more than 0.50 g g^{-1} soil [Figure 4(a) and (b)]. We interpreted this according to Sun *et al.*[19] and Bänninger *et al.*,[40] as

the result of interdependence among particle size, specific surface area of microaggregates and scattering angle.

L1 and L4 soils with porous massive structure and predominance of $\Phi_{250-1000}$ (Table 2) showed higher Fe_2O_3 and Al_2O_3 content compared to soils with cohesive massive structure (Table 1), and soils with predominance of microaggregates and higher content of Al and Fe usually have larger specific surface areas.[41]

The second effect is that of micro-organisation of microaggregates on the processes of light absorption and reflectance. When photon energy enters a particle, in this case a microaggregate, some is reflected by the surface of the microaggregate, some passes through the microaggregate and some is absorbed.[40,42] This process of reflection and/or absorption may be affected by the anisotropic reticular zones present in the microaggregates. Ferralsol microaggregates contain anisotropic reticular zones of approximately 800 µm,[43] which are increased by the interaction between organic matter and

Table 3. Significant Pearson correlation coefficients of proportion of microaggregates predominant in the sample ($\Phi_{250-1000}$) with spectral attributes (RI_{CIE}, I_{Ka} and I_{Gb}) and wavelengths (nm) of seven soil profiles ($n = 56$, $p < 0.05$).

	$\Phi_{250-1000}$
Spectral attributes	
RI_{CIE}	0.88
I_{Ka}	−0.82
I_{Gb}	−0.82
$I_{Ka}/(I_{Ka} + I_{Gb})$	0.77
Wavelengths	
401	0.57
436	0.77
440	0.72
530	0.77
546	0.80
550	0.74
650	
700	
845	0.56
850	0.57
870	0.59
901	0.62
931	0.62
951	0.62
1051	0.60
1302	0.66
1401	0.74
1903	0.76
2201	0.82
2236	0.82
2263	0.81
2300	0.81
2352	0.82
2430	0.83

Figure 4. Absorption intensity of (a) red index and (b) kaolinite and gibbsite ratio of spectral samples according to proportion of microaggregates $\Phi_{250-1000}$ ($n = 56$).

iron and aluminium oxy-hydroxides.[44] Thus, the interaction between the organic matter and iron and aluminium oxy-hydroxide in the sample promotes an anisotropic environment within the microaggregate that increases the process of scattering light and noise, weakening the signal of the spectra at 436 nm, 546 nm and 2236 nm with increase of $\Phi_{250-1000}$.

On another scale of microaggregate analysis, the interaction between organic matter and iron and aluminium oxy-hydroxides may increase the scattering light for spectra of soil with porous massive structure because this interaction causes a disorganisation in the arrangement (stacking) of the minerals, primarily by the following two mechanisms: (i) binding to the surface of other minerals by their edges, promoting a disorganised stacking of kaolinite,[43,45,46] and (ii)

the iron acting as a polycationic ligand for other molecules in the composition and internal organisation of microaggregates, this same concept also applying to gibbsite.[45] In this way, the porosity formed by a disorganisation in the arrangement of the primary minerals results in increased specific surface area and anisotropic reticular zones, increasing the probability of light being absorbed in internal microaggregate pores, as observed by Bänninger et al.[40]

Thus, with our soil sample collection, sieving of the samples did not prevent the different reflectance intensity of light and or concavity of the spectra, inherent to soils with porous and cohesive macromorphological features.

These results highlight the potential use of Vis-NIR spectroscopy in analyses of soil structure. In addition, given the inversely proportional relationship of microaggregates with soil density, we can suggest another way of analysing the structure and density of soils, directly from the spectra without the need for predictive models.

Soil morphology evaluation by spectral attributes

Spectral attributes were correlated with Ferralsol morphology. Absorption intensities of RI_{CIE} were distinct from the intensities of massive cohesive structure soils [Table 2 and Figure 4(a)] and samples of L1 and L4 soils exhibited greater variability in the kaolinite and gibbsite absorption ratio [Figure 4(b)] in the region 2200–2300 nm, emphasising the effect of surface roughness and of the organisation of minerals within the microaggregates, as mentioned above. Therefore, analysis of the effect of microaggregates on spectra can be performed for samples sieved through a 2.00 mm mesh using spectral attributes.

The relationship between RI_{CIE} and the proportion of $\Phi_{250-1000}$, which is associated with the disorganisation of minerals,

favoured the distinction of Ferralsols because the reflection provided by the relationship between these attributes was inherent for the nature of macrostructures of those soils [Figure 4(a)]. These results are consistent with those of Huete and Escadafal[47] and Bänninger *et al.*,[40,48] who reported that the absorption intensity and spectral composition of reflected energy may be used to describe the optical behaviour of soil due to the influence of its chemical and mineralogical composition and of the size, distribution and arrangement of microaggregates.

Notably, relationships between RI_{CIE} and the proportion of $\Phi_{250-1000}$ overlapped the relationship of this spectral attribute with hematite contents. This microaggregate class accounts for over 75% of RI_{CIE} variability in soils. Furthermore, cohesive massive structure soils such as L9 soil (27.35 g kg^{-1} hematite) exhibited lower RI_{CIE} absorption intensities than L5, L7, L8 and L11 soils (maximum hematite content of 12.57 g kg^{-1}) (Tables 1 and 2). Thus, the effect of size and roughness of microaggregates present in a sample on the spectra mentioned by White and Roth,[1] Escadafal *et al.*,[17] Escadafal[48] and Wu *et al.*[18] may be evaluated by the Φ parameter for Ferralsols and should be further studied for other types of soils.

Another important factor of the influence of microaggregates on the spectra is that the predominance of $\Phi_{250-1000}$ and the disorganisation of minerals may have a negative effect on the construction of predictive models because although these minerals do not prevent observation, these factors hinder the observation of correlations between spectral (RI_{CIE}, I_{Ka} and I_{Gb}) and soil (hematite, goethite, gibbsite and kaolinite content) attributes. Thus, the more pronounced the strong granular and very thin structure of microaggregates, the greater the noise in the spectra, and consequently the greater the variability of the spectra of these soils is likely to be. Chang *et al.*,[20] Brunet *et al.*[50] and Wu *et al.*[18] also reported that increasing the roughness of soil samples promoted an increase in noise in the spectra.

Increased noise in the spectra, promoted by the proportion of microaggregates in a soil sample and by the stacking porosity of goethite and gibbsite minerals, may partially explain the weak correlation observed between pure and soil minerals[37] and the coefficients below 0.6 in the construction of models to predict iron oxides.[51]

Using Φ and the soil spectra

Using samples of clayey Ferralsols, Volland-Tuduri *et al.*[34] developed the equation $\Phi_{<0.84} = 1.97(1/\text{bulk density}) - 1.52$, which relates inverse bulk density to the proportion of microaggregates with diameter <840 µm ($\Phi_{<840}$). Thus, we evaluated the effects of microaggregates on the spectra using the $\Phi_{<840}$ equation that represents the relationship between microaggregates and bulk density of other Ferralsols but in a pedologically and geomorphologically similar situation to this study.

The variation of RI_{CIE} and kaolinite and gibbsite ratio using the prediction results for $\Phi_{<840}$ was similar to that observed in this study when the proportion of $\Phi_{250-1000}$ was determined.
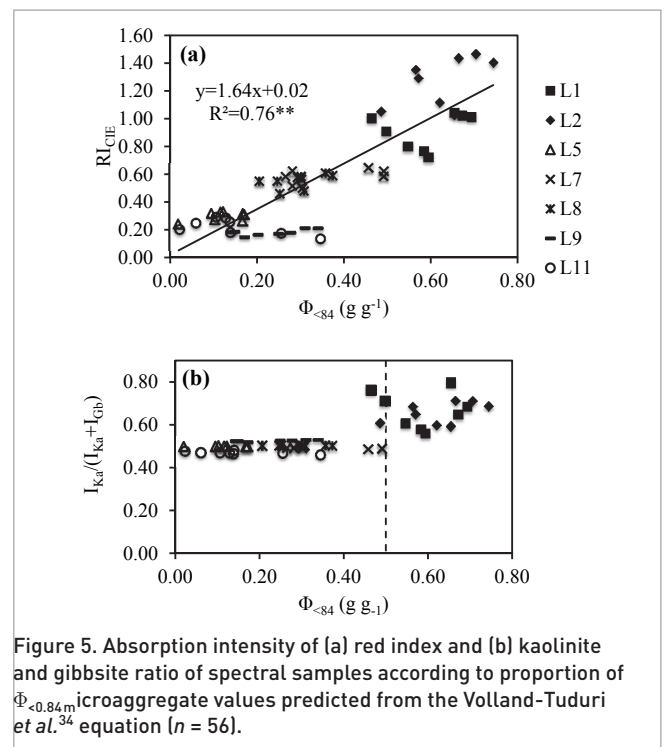
Figure 5. Absorption intensity of (a) red index and (b) kaolinite and gibbsite ratio of spectral samples according to proportion of $\Phi_{<0.84}$microaggregate values predicted from the Volland-Tuduri *et al.*[34] equation ($n = 56$).

Results obtained from the equation proposed by Volland-Tuduri *et al.*[34] were similar to the results obtained in the present study, despite the different classes of aggregates used. The difference in RI_{CIE} variation range and absorption intensity of gibbsite when kaolinite was constant could be observed according to the increased proportion of $\Phi_{<840}$ in the soil sample, particularly when this proportion was more than 0.50 g g^{-1} of soil microaggregates (Figure 5). This result confirmed the differences between the $\Phi_{250-1000}$ values of the porous massive structure and cohesive massive structure soils measured in this study (Table 2) and highlighted that the relationship between Φ and spectral attributes, RI_{CIE} and reflectance intensity of kaolinite and gibbsite content, may be extrapolated to other landscapes with Ferralsols whose characteristics are similar to those of this study.

The differences in I_{Ka} and I_{Gb} ratio between $\Phi_{250-1000}$ and $\Phi_{<840}$ when the proportion of microaggregates was less than 0.50 g g^{-1} of soil sample [Figures 4(b) and 5(b)] were due to the effect of the fine sand fraction of the samples. For our collection of samples, fractions smaller than 250 µm were related to the fine sand fraction ($R^2 = 0.70$, $p < 0.01$), which was composed of pseudo sand particles (microaggregates not dispersed during the analytical procedures with NaOH)[52] and of quartz, particularly for profiles with medium clayey texture, which was a texture not included in the Volland-Tuduri *et al.*[34] model.

Conclusions

Ferralsols with various macromorphological structures were characterised using the proportion of predominant soil

microaggregate mass (Φ). The predominant microaggregate diameter of these soils ranged between 250 µm and 1000 µm ($\Phi_{250-1000}$).

The results of this study allowed the millimetre- and micrometre-scale observation of the effect of the presence of aggregates with various sizes and composition on the spectra. The more pronounced the morphological porous massive structure with a strong granular and very thin structure of microaggregates, the greater the scattering and variability of the spectra of these soils. The microaggregate size explained over 55% of reflectance intensity variability of the wavelengths in the visible and NIR regions, principally of the reflectance intensity and the concavity of the spectra at 436 nm, 546 nm and 2236 nm that decreased with the increased proportion of $\Phi_{250-1000}$.

The 2 mm sieving of soil samples did not prevent the different reflectance intensity of light and or concavity of the spectra, which are different for soils with porous and cohesive morphological structures.

The CIE red index and the absorption intensity of kaolinite and gibbsite obtained from the Vis-NIR spectra can be used to characterise the morphological differences between Ferralsols. As well as spectra, the discrimination of Ferralsols can be performed through the spectral red index and absorption intensity of kaolinite and gibbsite, given the significant linear relationship between microaggregates and RI_{CIE} and the difference in variability of I_{Ka} and I_{Gb} ratio according to soil structures.

Acknowledgements

Conflict of interest

The authors have no conflicts of interest to declare.

References

1. J.L. White and C.B. Roth, "Infrared spectroscopy", in *Methods of Soil Analysis, Part I: Physical and Mineralogical Methods*, Ed by G.S. Campbell, R.D. Jackson, M.M. Mortland, D.R. Nielsen and A. Klute. American Society of Agronomy, Soil Science Society of America, Madison, WI, pp. 291–326 (1986).

2. C. Pasquini, "Near infrared spectroscopy: fundamentals, practical aspects and analytical applications", *J. Brazilian Chem. Soc.* **14,** 198 (2003). doi: http://dx.doi.org/10.1590/S0103-50532003000200006

3. B. Stenberg, R.A. Viscarra Rossel, A.M. Mouazen and J. Wetterlind, "Visible and near infrared spectroscopy in soil science", in *Advances in Agronomy*, Ed by D.L. Sparks. Academic Press, Burlington, MA, pp. 163–215 (2010).

4. K.H. Norris and J.R. Hart, "Direct spectrophotometric determination of moisture content of grain and seeds", in *Proceedings of the 1963 International Symposium on Humidity and Moisture*, New York, pp. 19–25 (1965).

5. I. Ben-Gera and K.H. Norris, "Direct spectrophotometric determination of fat and moisture in meat products", *J. Food Sci.* **33,** 64 (1968). doi: http://dx.doi.org/10.1111/j.1365-2621.1968.tb00885.x

6. WRB, *World Reference Base for Soil Resources*. FAO, Rome (2006).

7. H.G. Santos, P.K.T. Jacomine, L.H.C. Anjos, V.A. Oliveira, J.B. Oliveira, M.R. Coelho, J.F. Lumbrelas and T.J.F. Cunhas, *Sistema Brasileiro de Classificação de Solos*. Centro Nacional de Pesquisa de Solos, Rio de Janeiro (2006).

8. H. Neufeldt, M.A. Ayarza, D.V.S. Resck and W. Zech, "Distribution of water-stable aggregates and aggregating agents in Cerrado Oxisols", *Geoderma* **93,** 85 (1999). doi: http://dx.doi.org/10.1016/S0016-7061(99)00046-4

9. R. Westerhof, P. Buurman, C. van Griethuysen, M. Ayarza, L. Vilela and W. Zech, "Aggregation studied by diffraction in relation to plowing and liming in the Cerrado region in Brazil", *Geoderma* **90,** 277 (1999). doi: http://dx.doi.org/10.1016/S0016-7061(98)00133-5

10. M.L. Kubiena, "Zur micromorphologie der braunen und roten tropenboden", in *Transactions of the 4th International Congress of Soil Science*, Vol. 1, pp. 304–307 (1950).

11. R. Brewer, *Fabric and Mineral Analysis of Soils*. Wiley, New York (1964).

12. C.G. Trapnell, R. Webster and P.R. Hesse, "Microaggregates in red earths and related soils in East and Central Africa, their classification and occurrence", *J. Soil Sci.* **37,** 109 (1986). doi: http://dx.doi.org/10.1111/j.1365-2389.1986.tb00012.x

13. L.C. Balbino, A. Bruand, M. Brossard, M. Grimaldi, M. Hajnos and M.F. Guimarães, "Changes in porosity and microaggregation in clayey Ferralsols of the Brazilian Cerrado", *Eur. J. Soil Sci.* **53,** 219 (2002). doi: http://dx.doi.org/10.1046/j.1365-2389.2002.00446.x

14. M.M. Ferreira, B. Fernandes and N. Curi, "Mineralogia da Fração Argila e Estrutura de Latossolos da Região Sudeste do Brasil", *Revista Brasileira de Ciência do Solo* **23,** 507 (1999).

15. N. Volland-Tuduri, "Nature et mode d'assemblage des constituants minéraux et organiques dans des Ferralsols de la région des cerrados (Brésil): evolution après mise en culture", PhD thesis, Université D'Orléans (2005).

16. L.C. Balbino, M. Brossard, J.-C. Leprun and A. Bruand, "Mise en valeur des Ferralsols de la Région du Cerrado (Brésil) et évolution de leurs propriétés physiques: une étude bibliographique", *Étude et Gestion des Sols* **9,** 83 (2002).

17. R. Escadafal, C. Gouinaud, R. Mathieu and M. Pouget, "Le spectroradiomètre de terrain: un outil de la télé-détection et de la pédologie", *Cahiers Orstom, série Pédologie* **28,** 15 (1993).

18. C.Y. Wu, A.R. Jacobson, M. Laba and P.C. Baveye, "Accounting for surface roughness effects in the near infrared reflectance sensing of soils", *Geoderma* **152,** 171 (2009). doi: http://dx.doi.org/10.1016/j.geoderma.2009.06.002

19. Z. Sun, J.Z.Z. Tong and Y. Zhao, "Particle size effects on the reflectance and negative polarization of light backscattered from natural surface particulate medium: soil and sand", *J. Quant. Spectrosc. Radiat. Transf.* **133,** 1 (2014). doi: http://dx.doi.org/10.1016/j.jqsrt.2013.03.013

20. C.W. Chang, D.A. Laird, M.J. Mausbach and C.R. Hurburgh Jr, "Near-infrared reflectance spectroscopy – principal components regression analyses of soil properties", *Soil Sci. Soc. Am. J.* **65,** 480 (2001). doi: http://dx.doi.org/10.2136/sssaj2001.652480x

21. S. Chamizo, A. Stevens, Y. Cantón, I. Miralles, F. Domingo and B. Van Wesemael, "Discriminating soil crust type, development stage and degree of disturbance in semiarid environments from their spectral characteristics", *Eur. J. Soil Sci.* **63,** 42 (2012). doi: http://dx.doi.org/10.1111/j.1365-2389.2011.01406.x

22. H. Croft, K. Anderson and N.J. Kuhn, "Reflectance anisotropy for measuring soil surface roughness of multiple soil types", *Catena* **93,** 87 (2012). doi: http://dx.doi.org/10.1016/j.catena.2012.01.007

23. P. Jouquet, T. Henry-des-Tureaux, J. Mathieu, T.D. Thu, T.T. Duc and D. Orange, "Utilization of near infrared reflectance spectroscopy (NIRS) to quantify the impact of earthworms on soil and carbon erosion in steep slope ecosystem: a study case in northern Vietnam", *Catena* **81,** 113 (2010). doi: http://dx.doi.org/10.1016/j.catena.2010.01.010

24. J. Torrent, U. Schwertmann, H. Fechter and F. Alferez, "Quantitative relationships between soil color and hematite content", *Soil Sci.* **136,** 354 (1983). doi: http://dx.doi.org/10.1097/00010694-198312000-00004

25. J.S. Madeira Netto, A. Bedidi, B. Cervelle, M. Pouget and N. Flay, "Visible spectrometric indices of hematite (Hm) and goethite (Gt) content in lateritic soils: the application of a thematic mapper (TM) image for soil-mapping in Brasilia, Brazil", *Int. J. Remote Sens.* **18,** 2835 (1997). doi: http://dx.doi.org/10.1080/014311697217369

26. Z. Szalai, K. Kiss, G. Jakab, P. Sipos, B. Belucz and T. Németh, "The use of UV-VIS-NIR reflectance spectroscopy to identify iron minerals", *Astron. Nachr.* **334,** 940 (2013). doi: http://dx.doi.org/10.1002/asna.201211965

27. R.D. Santos, R.C. Lemos, H.G. Santos, J.C. Ker and L.H.C. Anjos, *Manual de Descrição e Coleta de Solo No Campo.* Sociedade Brasileira de Ciência do Solo, Viçosa (2005).

28. *Munsell Soil Color Charts.* Munsell Color Company, Baltimore, MD (1975).

29. J.F. Oliveira, M. Brossard, P.R.S. Vendrame, S. Mayi III, E.J. Corazza, R.L. Marchão and M.F. Guimarães, "Soil discrimination using diffuse reflectance Vis–NIR spectroscopy in a local toposequence", *C. R. Geosci.* **345,** 446 (2013). doi: http://dx.doi.org/10.1016/j.crte.2013.12.001

30. G.K. Donagema, D.V.B. Campos, S.B. Calderano, W.G. Teixeira and J.H.M. Viana, *Manual de Métodos de Análise de Solos.* Embrapa Solos, Rio de Janeiro (2011).

31. M. Resende, A.F.C. Bahia Filho and J.M. Braga, "Mineralogia da argila de latossolos estimada por alocação a partir do teor total de óxidos do ataque sulfúrico", *Revista Brasileira de Ciência do Solo* **11,** 17 (1987).

32. U. Schwertmann and R.M. Taylor, "Iron oxides", in *Minerals in Soil Environments*, Ed by J.B. Dixon and S.B. Weed. Soil Science Society of America, Madison, WI, pp. 379–438 (1989).

33. M. Resende and D.P. Santana, "Uso das relações Ki e Kr na estimativa da mineralogia para classificação dos latossolos", in *Anais da 3 Reunião de Classificação, Correlação de Solos e Interpretação de Aptidão Agrícola.* EMBRAPA–SNLCS/SECS, Rio de Janeiro, pp. 225–229 (1988).

34. N. Volland-Tuduri, A. Bruand, M. Brossard, L.C. Balbino, M.I.L. Oliveira and E.S. Martins, "Mass proportion of microaggregates and bulk density in a Brazilian clayey Oxisol", *Soil Sci. Soc. Am. J.* **69,** 1559 (2005). doi: http://dx.doi.org/10.2136/sssaj2003.0344

35. J.S. Madeira Netto, *Étude Quantitative des Relations Constituants Minéralogiques – Réflectance Diffuse des Latosols Brésiliens: Application à l'Utilisation Pédolocique des Données Satellitaires TM (Région de Brasilia).* Université Pierre et Marie Curie (Paris VI) (1993).

36. J.S. Madeira Netto, A. Bédidi, M. Pouget, B. Cervelle and N. Flay, "Spectral (MIR) determination of kaolinite and gibbsite contents in lateritic soils", *C. R. Acad. Sci.* **321,** 119 (1995). doi: http://dx.doi.org/1250-8050/95/03210119

37. R.A. Viscarra Rossel, R.N. Mcglynn and A.B. McBratney, "Determining the composition of mineral-organic mixes using UV–vis–NIR diffuse reflectance spectroscopy", *Geoderma* **137,** 70 (2006). doi: http://dx.doi.org/10.1016/j.geoderma.2006.07.004

38. J.A.M. Demattê and F.S. Terra, "Spectral pedology: a new perspective on evaluation of soils along pedogenetic alterations", *Geoderma* **217–218,** 190 (2014). doi: http://dx.doi.org/10.1016/j.geoderma.2013.11.012

39. P. Dalgaard, "Analysis of variance and the Kruskal–Wallis test", in *Statistics in Computing*, Springer, pp. 127-143 (2008). doi: http://dx.doi.org/10.1007/978-0-387-79054-1_7

40 D. Bänninger, P. Lehmann and H. Flühler, "Modelling the effect of particle size, shape and orientation of light transfer through porous media", *Eur. J. Soil Sci.* **57,** 906 (2006). doi: http://dx.doi.org/10.1111/j.1365-2389.2005.00787.x

41. C. Feller, E. Schouller, F. Thomas, J. Rouiller and A.J. Herbillon, "N2-BET specific surface areas of some low activity clay soils and their relationships with secondary constituents and organic matter contents", *Soil Sci.* **153,** 293 (1992).

42. R.N. Clark, "Reflectance spectra", in *Handbook of Physical Constants*. American Geophysical Union, Washington, DC, pp. 178–188 (1995).

43. G. Vrdoljak and G. Sposito, "Soil aggregate hierarchy in a Brazilian Oxisol", in *Developments in Soil Science*, Ed by A. Violante, P.M. Huang, J.-M. Bollag and L. Gianfreda. Elsevier Science, New York, pp. 197–217 (2002).

44. L. Gargiulo, G. Mele and F. Terribile, "Image analysis and soil micromorphology applied to study physical mechanisms of soil pore development: an experiment using iron oxides and calcium carbonate", *Geoderma* **197–198,** 151 (2013). doi: http://dx.doi.org/10.1016/j.geoderma.2013.01.008

45. E. Camacho, M. Robert and A.M. Jaunet, "Mineralogy and structural organization of a red to yellow soil sequence in Cuba. Relationship with soil properties", in *Proceedings of the VIIth International Working Meeting on Soil Micromorphology*, Paris, pp. 183–190 (1987).

46. O. Rozenbaum, A. Bruand and E.L. Trong, "Soil porosity resulting from the assemblage of silt grains with a clay phase: new perspectives related to utilization of X-ray synchrotron computed microtomography", *C. R. Geosci.* **344,** 516 (2012). doi: http://dx.doi.org/10.1016/j.crte.2012.09.004

47. A.R. Huete and R. Escadafal, "Assessment of biophysical soil properties through spectral decomposition techniques", *Remote Sens. Environ.* **35,** 149 (1991). doi: http://dx.doi.org/10.1016/0034-4257(91)90008-T

48. D. Bänninger and H. Flühler, "Modeling light scattering at soil surfaces", *IEEE Trans. Geosci. Remote Sens.* **42,** 1462 (2004). doi: http://dx.doi.org/10.1109/TGRS.2004.828190

49. R. Escadafal, "Remote sensing of arid soil surface color with Landsat thematic mapper", *Adv. Space Res.* **9,** 159 (1989). doi: http://dx.doi.org/10.1016/0273-1177(89)90481-X

50. D. Brunet, B.G. Barthès, J.-L. Chotte and C. Feller, "Determination of carbon and nitrogen contents in Alfisols, Oxisols and Ultisols from Africa and Brazil using NIRS analysis: effects of sample grinding and set heterogeneity", *Geoderma* **139,** 106 (2007). doi: http://dx.doi.org/10.1016/j.geoderma.2007.01.007

51. P.R.S. Vendrame, R.L. Marchão, D. Brunet and T. Becquer, "The potential of NIR spectroscopy to predict soil texture and mineralogy in Cerrado Latosols", *Eur. J. Soil Sci.* **63,** 743 (2012). doi: http://dx.doi.org/10.1111/j.1365-2389.2012.01483.x

52. J.B.V. Gomes, N. Curi, D.G. Schulze, J.J.G.S.M. Marques, J.C. Ker and P.E.F. Motta, "Mineralogia, morfologia e análise microscópica de solos do bioma cerrado", *Revista Brasileira de Ciência do Solo* **28,** 679 (2004).